Tunnel Passing Maneuvers of a Team of Car-like Robots in Formation

Bibhya SHARMA[1], Jito VANUALAILAI[1], Shin-Ichi NAKAGIRI[2] and Shonal SINGH[1]

1. University of the South Pacific, FIJI
2. Kobe University, JAPAN

Abstract

The research essays the design of a motion planner that will simultaneously manage collision and obstacle avoidances of a team of nonholonomic car-like robots fixed in prescribed formation and ensure desirable tunnel passing maneuvers. This decentralized planner, derived from the Lyapunov-based control scheme works within a leader-follower framework to generate either split/rejoin or expansion/contraction of the formation, as feasible solutions to the tunnel passing problem. In either scenario, the prescribed formation will be re-established after the tunnel has been passed. Moreover, avoidance of the walls of a tunnel will be accomplished via the minimum distance technique. The results can be viewed as a significant contribution to the intelligent vehicle systems discipline.

Keywords: Lyapunov-based control scheme; split/rejoin; expansion/contraction; formation control; tunnel passing.

Subject Classification 34D20; 37J60; 68T40; 70E60; 93C85; 93D05.

1 Introduction

The concept of formation control has in recent years garnered monumental attention from researcher all over, for both theoretical research and real-world applications. Formation control is basically to control the posture (position and orientation) of a team of agents while normally maintaining constant their relative locations and allowing them to travel to their desired destinations [1–5]. Formation control in difficult and constrained environments has been favored because of the wide spectrum of formation stiffness possible (eg. split/rejoin, low degree, rigid) and its relevancy to different real-life applications. The applications include surveillance; transportation; reconnaissance; save and rescue; pursuit-evasion; and exploration in either fully known or partially known environments, environments that may be very harsh, or hazardous, or even inaccessible to humans.

The literature harbors leader-follower, virtual structure, nearest neighbors, social potentials and the behavior based approaches to address the problem of formation control. Although each has its share of advantages and disadvantages, the leader- follower approach seems to be favored because of its simplicity and scalability [2, 6–8]. Furthermore, the approach has the ability to contain a wide range of formations with richer specifications and complexities. Generally, when the posture of the leader-robot is known, desired postures of the follower-robots can be achieved by appropriate control laws. However, the leader-follower approach is widely known for its poor disturbance rejection properties [2] and the dependence placed upon a single agent which can be crucial in atrocious and adverse conditions.

The main strength of this research lies in the emphasis placed upon the tunnel passing maneuvers, a practical situation commonly seen on our roads and highways. We take this tunnel passing problem to a higher level by considering formation control of a team of nonholonomic car-like robots through a tunnel. From the authors' viewpoint, although there are a number of techniques that can be successfully deployed to generate feasible algorithms of the tunnel passing problem, namely; scaling; prioritizing; caging [9]; split/rejoin [4, 16–18]; and contraction/expansion of the teams, only the latter two can possibly maintain the prescribed formations, at least, before and after tunnel passing. The two strategies are elegant, simple to implement and yet meet the expectations of the researcher. For the very first time we deploy the two techniques to solve this interesting but complicated problem within the overarching framework of a new control scheme.

Operations within the control scheme are guided by the principles of the Direct Method of Lyapunov, hence the control scheme is appropriately classified as a *Lyapunov-based control scheme* (LBCS), an artificial potential field method [19]. The reader is referred to [19] for a detailed account of the LbCS.

This paper is organized as follows: in Section 2 the car-like robot model is defined; in Section 3 the tunnel problem is designed and the two strategies are described; in Section 4 the attractive and repulsive potential field functions are designed and explained; in Section 5 the acceleration controllers are designed and stability of the robot system carried out; in Section 6 computer simulations of interesting scenarios are carried out; and Section 7 concludes the paper and outlines future work in the area.

2 Car-like Robot Model

Definition 1 *The ith front-wheel steered car-like mobile robot is a disk with radius r_{Vi} and is positioned at center (x_i, y_i). Precisely, the ith car-like robot is the set*

$$A_i = \{(z_1, z_2) \in \mathbb{R}^2 : (z_1 - x_i)^2 + (z_2 - y_i)^2 \leq r_{Vi}\},$$

where A_1 and A_i for $i = 2, \ldots, n$ are the lead robot and the follower-robots, respectively, of a team of nonholonomic car-like robots.

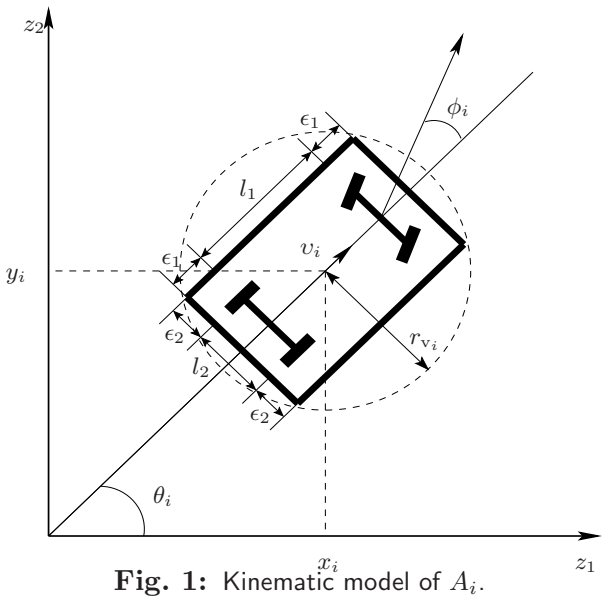

Fig. 1: Kinematic model of A_i.

With reference to Fig. 1, $[x_i, y_i]^T$ denotes the *CoM* of A_i, ϕ_i gives its steering wheel's angle with respect to the longitudinal axis, l_1 is the distance between the center of the rear and front axles, while l_2 is the length of each axle.

The configuration of A_i is given by $\boldsymbol{q}_i = [x_i, y_i, \theta_i]^T \in \mathbb{R}^3$, where $\boldsymbol{d}_i = [x_i, y_i]^T \in \mathbb{R}^2$ is its position and $\theta_i \in \mathbb{R}$ its angle with respect to z_1-axis.

If we let m_i be the mass of the robot, F_i the force along the axis of the robot, Γ_i the torque about a vertical axis at $[x_i, y_i]^T$ and I_i the moment of inertia of the robot, then the dynamic model of A_i with respect to its *CoM* is

$$\left.\begin{aligned} &\dot{x}_i = \upsilon_i \cos\theta_i - \frac{l_1}{2}\omega_i \sin\theta_i\,, \quad \dot{y}_i = \upsilon_i \sin\theta_i + \frac{l_1}{2}\omega_i \cos\theta_i\,, \\ &\dot{\theta}_i := \frac{\upsilon_i}{l_1}\tan\theta_i = \omega_i\,, \quad \dot{\upsilon}_i := F_i/m_i = \sigma_i\,, \quad \dot{\omega}_i := \Gamma_i/I_i = \eta_i\,, \end{aligned}\right\} \tag{1}$$

where υ_i and ω_i are, respectively, the instantaneous translational and rotational velocities, while σ_i and η_i are the instantaneous translational and rotational accelerations of A_i. In addition, we assume no slippage (i.e. $\dot{x}_i \sin\theta_i - \dot{y}_i \cos\theta_i = 0$) and pure rolling (i.e. $\dot{x}_i \cos\theta_i + \dot{y}_i \sin\theta_i = \upsilon_i$) of the wheels. These generate non-integrable constraints of the system, constraints that are passionately denoted as the nonholonomic constraints. We note that these constraints are already reflected in system (1). The dynamic constraints tagged to the system will be treated in a later section.

The state of robot A_i is captured in $\boldsymbol{x}_i = [x_i, y_i, \theta_i, \upsilon_i, \omega_i]^T \in \mathbb{R}^5$ and its acceleration controls in $\boldsymbol{u}_i = [\sigma_i, \eta_i]^T \in \mathbb{R}^2$. We collect the states of all the n robot in the vector $\boldsymbol{x} = [\boldsymbol{x}_1^T, \ldots, \boldsymbol{x}_n^T]^T \in \mathbb{R}^{5\times n}$ and the acceleration controls in $\boldsymbol{u} = [\boldsymbol{u}_1^T, ..., \boldsymbol{u}_n^T]^T \in \mathbb{R}^{2\times n}$.

Next, given the *clearance parameters* ϵ_1 and ϵ_2, we enclose each A_i in a protective circular region centered at $\boldsymbol{d}_i$ with radius $r_{\mathrm{v}} = \sqrt{(l_1 + 2\epsilon_1)^2 + (l_2 + 2\epsilon_2)^2}/2$ to maximize the free space and ensure an easier construction of the potential field functions [4, 19].

3 Devising the Tunnel Passing Problem

Definition 2 *Tunnel passing is a geometric problem of generating collision-free maneuvers of agents from arbitrary initial positions through a 2D-tunnel of given geometry.*

In this research, we drive a team of robots through a 2D-tunnel of given geometry. This tunnel passing problem can be divided into a number of sub-tasks: guiding the team in formation to the front of the tunnel; driving the team through the tunnel; and finally re-establishing the original formation of the team. We assume that the robots will be able to measure the distances from the tunnel walls using sensors.

Let us treat the top tunnel wall in the z_1z_2-plane as a line segment with initial coordinates (q_{11}, r_{11}) and final coordinates (q_{12}, r_{12}), while the bottom tunnel wall has initial and final coordinates as (q_{21}, r_{21}) and (q_{22}, r_{22}), respectively. Hence, we have region $t_f = \{0 < z_1 < q_{11}, r_{21} < z_2 < r_{11}\}$ and region $t_b = \{q_{22} < z_1, r_{22} < z_2 < r_{12}\}$. Therefore

Definition 3 *A point $\boldsymbol{z} \in \mathbb{R}^2$ is behind the tunnel if $\boldsymbol{z} \in t_b$ and is in front of the tunnel if $\boldsymbol{z} \in t_f$. The size of the tunnel entrance is denoted by h_t and it is a measure with reference to the z_2-axis.*

Definition 4 *h_f is the spread of the prescribed formation and it is a measure of the maximum inter-robot distance in relation to the z_2-axis.*

Assumption 1 *The team will be required to be fixed in a prescribed formation, at least, before and after the tunnel passing maneuver.*

Remark 1 *The assumption legislates a change in the formation to facilitate the passing maneuvers through the tunnel. This will be required when the size of the tunnel entrance will not allow the prescribed formation of the team to pass through, per se.*

In this research we will deploy contraction/expansion and split/rejoin of a team to provide feasible solutions to the tunnel passing problem. We will discuss each strategy in detail now.

3.1 Strategy I: Split/Rejoin of the Team

Definition 5 *Split/rejoin strategy is where multiple agents fixed in a specific formation split to steer past the encountering obstacle(s) and then rejoin to establish the prescribed formation.*

This research evokes the split/rejoin maneuver of a team of nonholonomic car-like mobile robots fixed in a formation in order to pass a tunnel of an arbitrary configuration. As illustrated in Figure 2(a), when $h_f + \epsilon > h_t$, the spread of the formation is greater than the size of the tunnel entrance, within a safety of ϵ, hence requiring split/rejoin. The split/rejoin maneuver, in the context of the tunnel passing problem, can be broken down into the following sub-tasks:

Sub-task 1: Drive the team into the prescribed formation;

Sub-task 2: Maintain the prescribed formation;

Sub-task 3: Steer the formation to the front entrance of the tunnel;

Sub-task 4: Activate the split maneuver of the team;

Sub-task 5: Drive the team members through the tunnel;

Sub-task 6: Activate the rejoin maneuver of the team to attain the prescribed formation within a maximum distance $d_0 \in t_b$. Note d_0 is measured relative to the leader position.

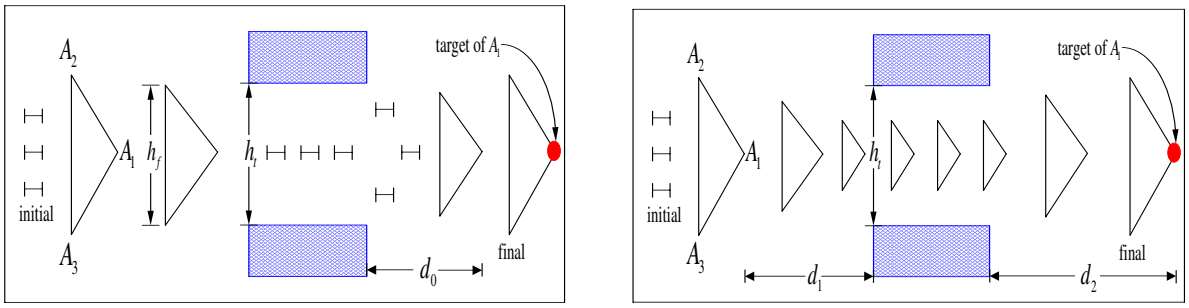

(a) Split/Rejoin

(b) Contraction/Expansion

Fig. 2: Schemes for the tunnel passing problem with A_1 as the leader robot.

3.2 Strategy II: Contraction/Expansion of the Team

Definition 6 *Contraction/expansion strategy is where the prescribed formation of the multiple agents is allowed to resize in order to steer past the encountering obstacle(s) and then return to the original size of the formation. Nonetheless, the prescribed shape is preserved throughout the journey.*

As illustrated in Figure 2(b), within a distance d_1, there has to be a successful contraction of the formation $h_f \Longrightarrow h_{f*}$ such that $h_{f*} + \epsilon < h_t$. It means that the spread of the formation is less than the size of the tunnel entrance, within a safety of ϵ. We will develop an algorithm which again involves six major sub-tasks:

Sub-task 1: Drive the team into the prescribed formation;

Sub-task 2: Maintain the prescribed formation;

Sub-task 3: Steer the formation to a distance of $d_1 \in t_f$. Note d_1 is measured relative to the leader position;

Sub-task 4: Activate the contraction maneuver of the team to reduce the size of the formation. Rate of contraction of formation will be relative to the h_f and h_t measures;

Sub-task 5: Drive the team fixed in the reduced size through the tunnel;

Sub-task 6: Activate the expansion maneuver of the team to attain the original size of the prescribed formation within a maximum distance $d_2 \in t_b$.

3.3 Control Objective

The overall control objective of this paper is to design decentralized acceleration controllers, σ_i and η_i, for each A_i in system (1), within the framework of LbCS, to navigate safely through the tunnel either from a split/rejoin or a contraction/expansion maneuver of a team in formation, within a finite period of time.

4 Artificial Potential Field Functions

In this section, we will construct attractive and repulsive potential field functions required to tackle each sub-task tagged to the split/rejoin and the contraction/expansion strategies. For simplicity we make the following assumption:

Assumption 2 *The dimensions, the maximum speed υ_{max} and the maximum steering angle ϕ_{max} of the n car-like robots are kept the same.*

We now look into the various aspects of the two strategies and carefully consider the associated potential field functions.

4.1 Drive the team into the prescribed formation

There are basically two phases of *Sub-task 1*: (1) initiate movement of the team members, and (2) establish the prescribed formation. We note that irrespective of the differences contained in the two strategies, the mathematical treatment of the two parts are the same for the two strategies. We shall consider these two parts separately.

4.1.1 Drive

To initiate movement we propose to have a target for each member of the team. Therefore, for A_i, we define a target $T_i = \{(x_i, y_i) \in \mathbb{R}^2 : (x_i - t_{i1})^2 + (y_i - t_{i2})^2 \leq rt_i^2\}$ with center (t_{i1}, t_{i2}) and radius rt_i. For each A_i to be attracted to T_i and its center finally positioned at (t_{i1}, t_{i2}) we utilize an attractive potential field function $U_{att} : \mathbb{R}^4 \to \mathbb{R}^+$ with

$$U_{att}(\boldsymbol{x}) = \sum_{i=1}^{n} H_{N_i}(\boldsymbol{x}) \tag{2}$$

where

$$H_{N_i}(\boldsymbol{x}) = \frac{1}{2}\ln(H_i + 1) \tag{3}$$

and the corresponding target attractive function is of the form

$$H_i(\boldsymbol{x}) = (x_i - t_{i1})^2 + (y_i - t_{i2})^2 + \upsilon_i^2 + \omega_i^2), \text{ for } i = 1, \ldots, n. \tag{4}$$

While the function is the measure of the distance between A_i and the target T_i, it can also be treated as a measure of convergence. This invariably substantiates the first phase of *Sub-task 1*.

4.1.2 Establish Prescribed Formation

To realize the second phase of *Sub-task 1* we adopt the leader-follower scheme described by Sharma *et al.* in [4]. The scheme was designed to navigate a flock in a constrained environment. This elegant yet simple scheme will be instrumental in establishing the prescribed formation of the team, for either strategy. In the scheme, see Figure 3, the follower robots follow the lead robot via *mobile ghost targets*. The ith mobile ghost target is positioned relative to the position of the lead robot.

This is a user-defined Euclidean measure of a_i units right or left and b_i units up or down, while the center of the ghost target is given by $(t_{i1}, t_{i2}) = (x_1 - a_i, y_1 - b_i)$, for $i = 2$ to n.

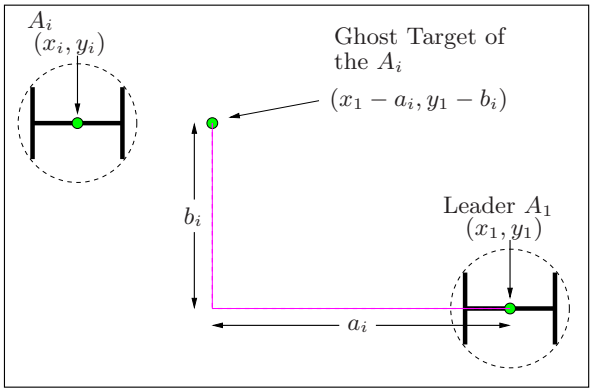

Fig. 3: The mobile ghost target for A_i relative to that of the leader.

As the lead robot A_1 moves towards its target T_1, the mobile ghost targets will move relative to the position of the lead robot.

In turn each follower-robot of the team moves towards a designated mobile ghost target at every iteration $t > 0$, hence establishing the prescribed formation [4]. A specific and prescribed formation can be established with appropriate values of the Euclidean measures a_i and b_i.

Figure 4 shows the potential valleys created by the attractive forces in a continuous potential field in relation to the moving ghost targets. The ultimate goal is for each robot to move to its designated valley (mobile ghost target) via steepest descent of the potential gradient.

4.2 Maintain the Prescribed Formation

To realize *Sub-task 2*, we design specific modules that govern the prescribed formation of the team. We note that these modules will greatly differ for the two strategies since we will want to activate two significantly different maneuvers to engender tunnel passing.

While for Strategy I the leader-follower scheme and the attractive potentials governed by equation (2) are sufficient to maintain the prescribed formation, the following bounds are enacted specifically for Strategy II to maintain a continued cohesion of the robots.

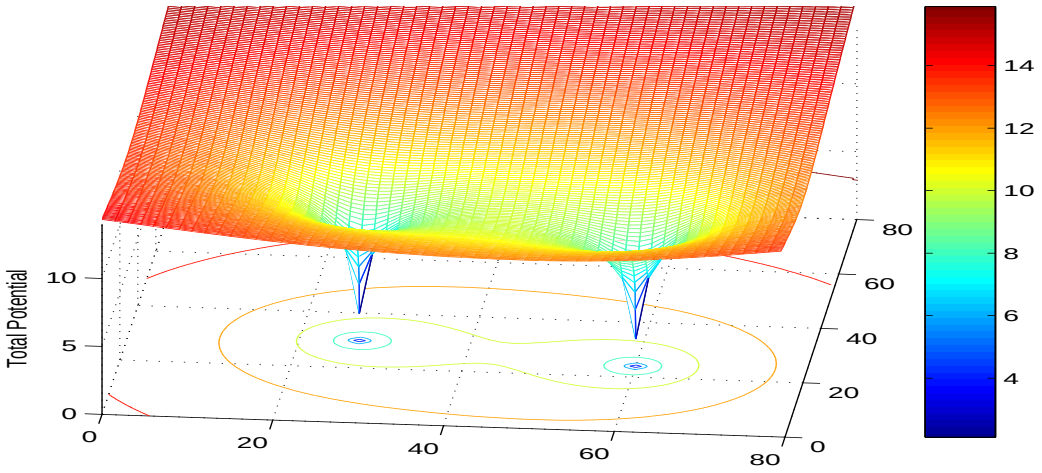

Fig. 4: Total potentials and the corresponding contour plot generated using the target attractive function governed by equation (2). The ghost targets are fixed at $(60, 24)$ and $(27, 30)$.

4.2.1 Maximum Inter-robot Bound

The maximum distance between any two robots of the team needs to be bounded so that a robot cannot drift off the prescribed formation. We thus desire a bound $\| \mathbf{d}_i - \mathbf{d}_j \|^2 < M_{ij}^2$ where M_{ij} is the maximum Euclidian distance between A_i and A_j on $\mathbb{R}^2$.

The only way this bound could be treated within the LbCS framework is to develop an *artificial obstacle* for it. We can choose $AO_{1ij} = \{\boldsymbol{x} \in \mathbb{R}^2 : (x_i - x_j)^2 + (y_i - y_j)^2 \geq M_{ij}^2\}$. To ensure that each robot of the team operates within these bounds, we need only avoid the corresponding artificial obstacles by appropriate repulsive potential field functions. Hence, we introduce tuning parameter $\zeta_{ij} > 0$, and adopt potential fields defined by $U_{rep_1} : \mathbb{R}^2 \to \mathbb{R}^+$ with

$$U_{rep_1}(\boldsymbol{x}) = \sum_{i=1}^{n} \sum_{\substack{j=1 \\ j \neq i}}^{n} \frac{\zeta_{ij}}{R_{ij}(\boldsymbol{x})} \tag{5}$$

where the obstacle avoidance function is of the form

$$R_{ij}(\boldsymbol{x}) = \frac{1}{2}\left[M_{ij}^2 - \{(x_i - x_j)^2 + (y_i - y_j)^2\}\right], \quad \text{for } i, j \in \{1, 2, \ldots, n\},\ j \neq i. \tag{6}$$

4.2.2 Minimum Inter-robot bound

The minimum inter-robot bounds prevent a robot from getting very close to (or colliding with) another robot. We desire the bound $\| \mathbf{d}_i - \mathbf{d}_j \|^2 > N_{ij}^2$ where N_{ij} is the minimum Euclidian distance given as $(r_V + r_V)^2 = 4r_V^2$ on $\mathbb{R}^2$. We can choose to have an *artificial obstacle* $AO_{2ij} = \{\boldsymbol{x} \in \mathbb{R}^2 : (x_i - x_j)^2 + (y_i - y_j)^2 \leq N_{ij}^2 = 4r_V^2\}$. For avoidance we introduce tuning parameter $\xi_{ij} > 0$, and adopt repulsive potential fields defined by $U_{rep_2} : \mathbb{R}^2 \to \mathbb{R}^+$

with

$$U_{rep_2}(\boldsymbol{x}) = \sum_{i=1}^{n} \sum_{\substack{j=1 \\ j \neq i}}^{n} \frac{\xi_{ij}}{MO_{ij}(\boldsymbol{x})} \tag{7}$$

where the obstacle avoidance function is of the form

$$MO_{ij}(\boldsymbol{x}) = \frac{1}{2}\left[(x_i - x_j)^2 + (y_i - y_j)^2 - 4r_V^2\right], \text{ for } i, j \in \{1, 2, \ldots, n\},\ j \neq i. \tag{8}$$

4.3 Drive Team to Front Entrance

In either strategy, to realize *Sub-task 3* we simply ensure that the team is driven towards the tunnel. It is easy to accept that we basically require $T_1 \in t_b$. As the lead robot approaches the tunnel entrance, the follower-robots follow their mobile ghost targets and hence also approach the front entrance.

4.4 Drive Team through the Tunnel

Sub-task 5 of either strategy addresses the ultimate goal of this research. This is to attain the tunnel passing maneuver and to make sure that all the team members are able to safely steer through the tunnel.

Since $T_1 \in t_b$ the target attractive functions constructed in Section 4.3 are sufficient to drive the team members through the tunnel. However, to garner an overall success, we need to address an important issue inherently tagged to *Sub-task 5*: obstacle and collision avoidances. We will now address the various avoidances deemed important to this sub-task.

4.4.1 Fixed Obstacles: Tunnel Walls

We assume that the walls of the tunnel are fixed obstacles that need to be avoided in either strategy while passing through. This also ensures containment of the motion within the walls of the tunnel.

Definition 7 *The kth tunnel wall is collapsed into a line segment in the z_1z_2-plane with initial coordinates (q_{k1}, r_{k1}) and final coordinates (q_{k2}, r_{k2}). The parametric representation of the kth tunnel wall can be given as $x_k = q_{k1} + \lambda_k(q_{k2} - q_{k1})$ and $y_k = r_{k1} + \lambda_k(r_{k2} - r_{k1})$ where $\lambda_k : \mathbb{R}^2 \to [0, 1]$.*

We will adopt the minimum distance technique (MDT) from [19] to facilitate the avoidance of these line segments. We calculate the minimum Euclidian distance from the center of A_i to the kth line segment and avoid the resultant point of the line segment. From geometry, coordinates of this point can be given as $x_{ik} = q_{k1} + \lambda_{ik}(q_{k2} - q_{k1})$ and $y_{ik} = r_{k1} + \lambda_{ik}(r_{k2} - r_{k1})$ where $\lambda_{ik} = (x_i - q_{k1})c_k + (y_i - r_{k1})d_k$,

$$c_k = \frac{(q_{k2} - q_{k1})}{(q_{k2} - q_{k1})^2 + (r_{k2} - r_{k1})^2}\ , \qquad d_k = \frac{(r_{k2} - r_{k1})}{(q_{k2} - q_{k1})^2 + (r_{k2} - r_{k1})^2}$$

and the saturation function is given by

$$\lambda_{ik}(x_i, y_i) = \begin{cases} 0 & , \text{ if } \lambda_{ik} < 0 \\ \lambda_{ik} & , \text{ if } 0 \leq \lambda_{ik} \leq 1 \\ 1 & , \text{ if } \lambda_{ik} > 1 \end{cases}$$

We note that $\lambda_{ik}(x_i, y_i)$ is a nonnegative scalar such that it is restricted to the interval $[0, 1]$. Hence, there is always an avoidance of the kth tunnel wall at every iteration $t \geq 0$. For example, $\lambda_{ik} = 0$ would mean that $A_i \in t_f$ and the point closest to it will be (q_{k1}, r_{k1}) which the robot has to avoid. Now, for each robot to avoid the closest point on each of the kth tunnel wall we introduce tuning parameter $\alpha_{ik} > 0$, for $i = 1$ to n and $k = 1, 2$, and consider repulsive potential fields defined by $U_{rep_3} : \mathbb{R}^2 \to \mathbb{R}^+$ with

$$U_{rep_3}(\boldsymbol{x}) = \sum_{i=1}^{n} \sum_{k=1}^{2} \frac{\alpha_{ik}}{W_{ik}(\boldsymbol{x})}, \tag{9}$$

where the associated obstacle avoidance function is of the form

$$W_{ik}(\boldsymbol{x}) = \frac{1}{2} \left\{ [x_i - (q_{k1} + \lambda_{ik}(q_{k2} - q_{k1}))]^2 + [y_i - (r_{k1} + \lambda_{ik}(r_{k2} - r_{k1}))]^2 - r_{\text{v}}^2 \right\}\ , \tag{10}$$

4.4.2 Moving Obstacles: Car-like Mobile Robots

While the minimum inter-robot bounds designed in Section 4.2.2 govern the formation of the team in Strategy II, they will also prevent inter-robot collisions.

We now need to address the collision avoidance issue for Strategy I. This is because once the team members are split there is a possibility that they can collide amongst each other, that is, each robot itself becomes a moving obstacle for all the other robots. For this we will simply deploy the repulsive potential field function given by equation (7) in Section 4.2.2 which will *also* prevent all possible inter-robot collisions.

4.5 Split/Rejoin and Contraction/Expansion Maneuver

Sub-task 4 and *Sub-task 6* involve activating the split/rejoin and contraction/expansion maneuvers of the team for Strategy I and Strategy II, respectively. While the lack of strong constraints help attain split/rejoin maneuvers in Strategy I, we will require the following updating rule to engender contraction/expansion of the formation in Strategy II:

$$a_i(t+1) = \begin{cases} -\rho_1 \left(a_i(0) - a_i^*\right) + a_i(t)\ , & \text{if } \lambda_{1k}(x_1, y_1) < 0, \\ a_i^* & , \text{ if } 0 \leq \lambda_{1k}(x_1, y_1) \leq 1, \\ -\rho_2 \left(a_i^* - a_i(0)\right) + a_i(t)\ , & \text{if } \lambda_{1k}(x_1, y_1) > 1, \end{cases}$$

and

$$b_i(t+1) = \begin{cases} -\rho_1 \left(b_i(0) - b_i^*\right) + b_i(t) \ , & \text{if } \lambda_{1k}(x_1, y_1) < 0, \\ b_i^* \ , & \text{if } 0 \leq \lambda_{1k}(x_1, y_1) \leq 1, \\ -\rho_2 \left(b_i^* - b_i(0)\right) + b_i(t) \ , & \text{if } \lambda_{1k}(x_1, y_1) > 1, \end{cases}$$

where the distance measures, a_i and b_i, will be iteratively updated from the attractive potential field function governed by equation (4) and from the saturation function $\lambda_{1k}(x_1, y_1)$ defined in Subsection 4.4. When $\lambda_{1k}(x_1, y_1) < 0$, $A_1 \in t_f$ which implies that the contraction $h_f \Longrightarrow h_{f*}$ continues such that $h_{f*} + \epsilon < h_t$. However, if $A_1 \in t_b$ then we continue to expand the formation, until the original size is re-established. This also establishes that the feedback gains $\rho_1, \rho_2 \in \mathbb{R}^+$ are directly dependent on distances d_1 and d_2. Furthermore, the critical measures to allow tunnel passing $a_i^* > 2 \times r_V$, and $b_i^* > 2 \times r_V$ need to be observed to avoid saturations.

4.6 Other Requirements

4.6.1 Auxiliary Function

To ensure that the total potentials vanish when the team converges to the final target configuration we design an auxiliary function defined by $U_{aux} : \mathbb{R}^3 \to \mathbb{R}^+$ with

$$U_{aux} = \sum_{i=1}^{n} G_i(\mathbf{x}) \tag{11}$$

where

$$G_i(\boldsymbol{x}) = \frac{1}{2} \left[(x_i - t_{i1})^2 + (y_i - t_{i2})^2 + (\theta_i - t_{i3})^2 \right] \ , \tag{12}$$

for $i = 1$ to n, where t_{i3} is the desired orientation of A_i.

4.6.2 Artificial Obstacles: Dynamics Constraints

In practice, the translational speed and the steering angle of the car-like robots are limited. If $\upsilon_{max} > 0$ and $0 < \phi_{max} < \frac{\pi}{2}$ then the constraints imposed on the translational and the rotational velocities are, respectively, $|\upsilon_i| < \upsilon_{max}$ and $|\omega_i| < \frac{\upsilon_{max}}{|\rho_{min}|}$ where $\rho_{min} = l_1 / \tan \phi_{max}$. Again, the only way these dynamic constraints could be treated within the LbCS framework is to develop an *artificial obstacle* for each. Hence we have:

$$AO_{3i1} = \{\upsilon_i \in \mathbb{R} : \upsilon_i \leq -\upsilon_{\max} \text{ or } \upsilon_i \geq \upsilon_{\max}\},$$
$$AO_{3i2} = \{\omega_i \in \mathbb{R} : \omega_i \leq -\upsilon_{\max}/|\rho_{\min}| \text{ or } \omega_i \geq \upsilon_{\max}/|\rho_{\min}|\}.$$

To avoid these artificial obstacles we introduce tuning parameter $\beta_{im} > 0$, for $i = 1$ to n and $m = 1, 2$, and use the repulsive potential fields defined by $U_{rep_4} : \mathbb{R}^2 \to \mathbb{R}^+$ with

$$U_{rep_4} = \sum_{i=1}^{n} \sum_{m=1}^{2} \frac{\beta_{im}}{U_{im}(\mathbf{x})} \tag{13}$$

where the associated avoidance functions are of the form

$$U_{i1}(\boldsymbol{x}) = \frac{1}{2}(\upsilon_{max} - \upsilon_i)(\upsilon_{max} + \upsilon_i) \tag{14}$$

$$U_{i2}(\boldsymbol{x}) = \frac{1}{2}\left(\frac{\upsilon_{max}}{|\rho_{min}|} - \omega_i\right)\left(\frac{\upsilon_{max}}{|\rho_{min}|} + \omega_i\right) \tag{15}$$

5 Controller Design and Stability Issues

The total attractive and repulsive APFs for system (1) are defined by $U_{att}(\mathbf{x})$ and $U_{rep}(\mathbf{x}) = \sum_{j=1}^{4} U_{rep_j}$, respectively. The resulting total force for system (1) is $F(\mathbf{x}) : \mathbb{R}^2 \rightarrow \mathbb{R}^2$ with

$$F(\mathbf{x}) = -\left(\bigtriangledown U_{att}(\mathbf{x}) + U_{rep}(\mathbf{x}) \times \bigtriangledown U_{aux}(\mathbf{x}) + U_{aux}(\mathbf{x}) \times \bigtriangledown U_{rep}(\mathbf{x})\right) \tag{16}$$

The collision-free trajectories are harvested following the notion of steepest descend. We begin with the following theorem:

Theorem 1 *Consider a team of car-like mobile robots, the motion of which is governed by ODEs described by system (1). The objective is to, amongst considering other integrated subtasks, establish and control a prescribed formation, facilitate tunnel passing maneuvers of the robots within a constrained environment and attain the target configuration in its original formation. Utilizing the potential field functions the following continuous time-invariant acceleration control laws can be generated for A_i that per se guarantees stability, in the sense of Lyapunov, of system (1) as well:*

$$\sigma_i = -\left[\delta_{i1}\upsilon_i + f_{1i}\cos\theta_i + f_{2i}\sin\theta_i\right]/f_{4i}\ , \tag{17}$$

$$\eta_i = -\left[\delta_{i2}\omega_i + \frac{l_l}{2}\left(f_{2i}\cos\theta_i - f_{1i}\sin\theta_i\right) + f_{3i}\right]/f_{5i}\ , \tag{18}$$

for $i = 1$ to n where $\delta_{i1}, \delta_{i2} > 0$ are constants commonly known as convergence parameters.

Remark 2 *The generalized controls are applicable to both strategies. Strategy that does not require a particular repulsive potential function will have a zero value of the corresponding control parameter.*

Proof:

We propose a Lyapunov function candidate for system (1):

$$L(\boldsymbol{x}) = \sum_{i=1}^{n}\left\{H_{N_i}(\boldsymbol{x}) + G_i(\boldsymbol{x})\left[\sum_{\substack{j=1\\ j\neq i}}^{n}\left(\frac{\zeta_{ij}}{R_{ij}(\boldsymbol{x})} + \frac{\xi_{ij}}{MO_{ij}(\boldsymbol{x})}\right) + \sum_{k=1}^{2}\frac{\alpha_{ik}}{W_{ik}(\boldsymbol{x})} + \sum_{m=1}^{2}\frac{\beta_{im}}{U_{im}(\boldsymbol{x})}\right]\right\}. \tag{19}$$

Assumption 3 *The point* $\boldsymbol{x}^* = (t_{11}, t_{12}, t_{13}, 0, 0, \ldots, t_{n1}, t_{n2}, t_{n3}, 0, 0) \in \mathbb{R}^{5\times n} \in D(L)$ *is an equilibrium point of system (1).*

Then one can easily verify that L is continuous and positive on the domain $\mathbb{D}$, $L(\boldsymbol{x}^*) = 0$, $\boldsymbol{x}^* \in \mathbb{D}$ and $L(\boldsymbol{x}) > 0 \quad \forall\ \boldsymbol{x} \in \mathbb{D}, \boldsymbol{x} \neq \boldsymbol{x}^*$. Now let us consider the first derivatives of the Cartesian quantities of our Lyapunov function candidate $L(\boldsymbol{x})$. Along a particular trajectory of system (1), we have, upon collecting terms with υ_i and ω_i separately

$$\dot{L}_{(1)}(\boldsymbol{x}) = \sum_{i=1}^{n} \left[\left(f_{1i}\cos\theta_i + f_{2i}\sin\theta_i + f_{4i}\sigma_i\right)\upsilon_i - \left(\frac{l_1}{2} f_{1i}[\sin\theta_i - f_{2i}\cos\theta_i] - f_{3i} - f_{5i}\eta_i\right)\omega_i \right] ,$$

where functions f_{1i} to f_{5i} are defined as (on suppressing $\boldsymbol{x}$):

$$\begin{aligned}
f_{11} &= \left(\frac{1}{H_1+1} + \sum_{k=1}^{2}\frac{\alpha_{1k}}{W_{1k}} + \sum_{m=1}^{2}\frac{\beta_{1m}}{U_{1m}} + \sum_{j=1,j\neq i}^{n}\left(\frac{\zeta_{1j}}{R_{1j}} + \frac{\xi_{1j}}{MO_{1j}}\right)\right)(x_1 - t_{11}) \\
&- \sum_{i=2}^{n}\left(\frac{1}{H_i+1} + \sum_{k=1}^{2}\frac{\alpha_{ik}}{W_{ik}} + \sum_{m=1}^{2}\frac{\beta_{im}}{U_{im}} + \sum_{j=1,j\neq i}^{n}\left(\frac{\zeta_{ij}}{R_{ij}} + \frac{\xi_{ij}}{MO_{ij}}\right)\right)(x_i - t_{i1}) \\
&+ G_1\sum_{j=1,j\neq i}^{n}\left(\frac{\zeta_{1j}}{R_{1j}^2} - \frac{\xi_{1j}}{MO_{1j}^2}\right)(x_1 - x_j) + \sum_{j=1,j\neq i}^{n} G_j\left(\frac{\xi_{j1}}{MO_{j1}^2} - \frac{\zeta_{j1}}{R_{j1}^2}\right)(x_j - x_1) \\
&- G_1\sum_{k=1}^{2}\frac{\alpha_{1k}}{W_{1k}^2}(x_1 - (q_{k1} + \lambda_{1k}(q_{k2} - q_{k1})))(1 - c_k(q_{k2} - q_{k1})) \\
&+ G_1\sum_{k=1}^{2}\frac{\alpha_{1k}}{W_{1k}^2}c_k(r_{k2} - r_{k1})(y_1 - (r_{k1} + \lambda_{1k}(r_{k2} - r_{k1}))).
\end{aligned}$$

$$\begin{aligned}
f_{21} &= \left(\frac{1}{H_1+1} + \sum_{k=1}^{2}\frac{\alpha_{1k}}{W_{1k}} + \sum_{m=1}^{2}\frac{\beta_{1m}}{U_{1m}} + \sum_{j=1,j\neq i}^{n}\left(\frac{\zeta_{1j}}{R_{1j}} + \frac{\xi_{1j}}{MO_{1j}}\right)\right)(y_1 - t_{12}) \\
&- \sum_{i=2}^{n}\left(\frac{1}{H_i+1} + \sum_{k=1}^{2}\frac{\alpha_{ik}}{W_{ik}} + \sum_{m=1}^{2}\frac{\beta_{im}}{U_{im}} + \sum_{j=1,j\neq i}^{n}\left(\frac{\zeta_{ij}}{R_{ij}} + \frac{\xi_{ij}}{MO_{ij}}\right)\right)(y_i - t_{i2}) \\
&+ G_1\sum_{j=1,j\neq i}^{n}\left(\frac{\zeta_{1j}}{R_{1j}^2} - \frac{\xi_{1j}}{MO_{1j}^2}\right)(y_1 - y_j) + \sum_{j=1,j\neq i}^{n} G_j\left(\frac{\xi_{j1}}{MO_{j1}^2} - \frac{\zeta_{j1}}{R_{j1}^2}\right)(y_j - y_1) \\
&- G_1\sum_{k=1}^{2}\frac{\alpha_{1k}}{W_{1k}^2}(y_1 - (r_{k1} + \lambda_{1k}(r_{k2} - r_{k1})))(1 - d_k(r_{k2} - r_{k1})) \\
&+ G_1\sum_{k=1}^{2}\frac{\alpha_{1k}}{W_{1k}^2}d_k(q_{k2} - q_{k1})(x_1 - (q_{k1} + \lambda_{1k}(q_{k2} - q_{k1}))).
\end{aligned}$$

For $i = 2$ to n

$$
\begin{aligned}
f_{1i} &= \left(\frac{1}{H_i+1} + \sum_{k=1}^{2}\frac{\alpha_{ik}}{W_{ik}} + \sum_{m=1}^{2}\frac{\beta_{im}}{U_{im}} + \sum_{j=1,j\neq i}^{n}\left(\frac{\zeta_{ij}}{R_{ij}} + \frac{\xi_{ij}}{MO_{ij}}\right)\right)(x_i - t_{11}) \\
&+ G_i \sum_{j=1,j\neq i}^{n}\left(\frac{\zeta_{ij}}{R_{ij}^2} - \frac{\xi_{ij}}{MO_{ij}^2}\right)(x_i - x_j) + \sum_{j=1,j\neq i}^{n} G_j\left(\frac{\xi_{ji}}{MO_{ji}^2} - \frac{\zeta_{ji}}{R_{ji}^2}\right)(x_j - x_i) \\
&- G_i \sum_{k=1}^{2}\frac{\alpha_{ik}}{W_{ik}^2}(x_i - (q_{k1} + \lambda_{ik}(q_{k2} - q_{k1})))(1 - c_k(q_{k2} - q_{k1})) \\
&+ G_i \sum_{k=1}^{2}\frac{\alpha_{ik}}{W_{ik}^2}c_k(r_{k2} - r_{k1})(y_i - (r_{k1} + \lambda_{ik}(r_{k2} - r_{k1}))), \\
f_{2i} &= \left(\frac{1}{H_i+1} + \sum_{k=1}^{2}\frac{\alpha_{ik}}{W_{ik}} + \sum_{m=1}^{2}\frac{\beta_{im}}{U_{im}} + \sum_{j=1,j\neq i}^{n}\left(\frac{\zeta_{ij}}{R_{ij}} + \frac{\xi_{ij}}{MO_{ij}}\right)\right)(y_i - t_{i2}) \\
&+ G_i \sum_{j=1,j\neq i}^{n}\left(\frac{\zeta_{ij}}{R_{ij}^2} - \frac{\xi_{ij}}{MO_{ij}^2}\right)(y_i - y_j) + \sum_{j=1,j\neq i}^{n} G_j\left(\frac{\xi_{ji}}{MO_{ji}^2} - \frac{\zeta_{ji}}{R_{ji}^2}\right)(y_j - y_i) \\
&- G_i \sum_{k=1}^{2}\frac{\alpha_{ik}}{W_{ik}^2}(y_i - (r_{k1} + \lambda_{ik}(r_{k2} - r_{k1})))(1 - d_k(r_{k2} - r_{k1})) \\
&+ G_i \sum_{k=1}^{2}\frac{\alpha_{ik}}{W_{ik}^2}d_k(q_{k2} - q_{k1})(x_i - (q_{k1} + \lambda_{ik}(q_{k2} - q_{k1}))).
\end{aligned}
$$

For $i = 1$ to n

$$
\begin{aligned}
f_{3i} &= \left(\sum_{k=1}^{2}\frac{\alpha_{ik}}{W_{ik}} + \sum_{m=1}^{2}\frac{\beta_{im}}{U_{im}} + \sum_{j=1,j\neq i}^{n}\left(\frac{\zeta_{ij}}{R_{ij}} + \frac{\xi_{ij}}{MO_{ij}}\right)\right)(\theta_i - t_{i3}) \ , \\
f_{4i} &= \frac{1}{H_i+1} + G_i\frac{\beta_{i1}}{U_{i1}^2} \ , \quad f_{5i} = \frac{1}{H_i+1} + G_i\frac{\beta_{i2}}{U_{i2}^2}.
\end{aligned}
$$

Substituting the controllers given in (17) - (18) and the governing ODEs for system (1) we obtain a semi-negative definite function

$$
\dot{L}_{(1)}(\boldsymbol{x}) = -\sum_{i=1}^{n}\left(\delta_{i1}\upsilon_i^2 + \delta_{i2}\omega_i^2\right) \leq 0 \ .
$$

We have thus provided a working proof of the fact that $\frac{d}{dt}[L(\boldsymbol{x})] \leq 0 \ \ \forall\, \boldsymbol{x} \in \mathbb{D}$.

Finally, it can easily be verified that the first partial's of $L_{(1)}(\boldsymbol{x})$ is C^1 which satisfies the final property of a Lyapunov function. Hence $L(\boldsymbol{x})$ is a feasible Lyapunov function for system (1) and $\boldsymbol{x}^*$ is a stable equilibrium point in the sense of Lyapunov. In our case, this practical limitation is well within the framework of the Lyapunov-based control scheme and there is no contradiction with Brockett's Theorem.

6 Computer Simulations

In this section we illustrate the effectiveness of the Lyapunov-based control scheme vis-a-vis the continuous time-invariant control laws, by simulating two interesting scenarios. We verify numerically the stability and the convergence results obtained from the control scheme. We present tunnel passing maneuver of a 3-robot team whereby each robot starts from an arbitrary position as depicted in Figure 2(a) and Figure 2(b). The teams get into the prescribed formations and translate to the front entrance of the tunnel. Split/rejoin and contraction/expansion maneuvers are carried out to facilitate tunnel passing. The original formations are established within a specified period of time after passing the tunnel.

6.1 Scenario 1: Split/Rejoin

Assuming the units have been appropriately taken care of, initial conditions of the 3-robot team, obstacles and target configurations, limitations on velocities, and values of different parameters are given in Table 1. We witness the split/rejoin maneuver of the team in order to

Table 1: Numerical values of initial states, constraints and parameters for a simulation of Scenario 1.

	Initial Conditions
Positions	$(x_1, y_1) = (5, 10), \quad (x_2, y_2) = (5, 15), \quad (x_3, y_3) = (5, 5).$
Velocities	$\theta_i = 0, \;\; \upsilon_i = 0.5, \quad \omega_i = 0, \quad$ for $i = 1$ to 3.
	Constraints and Parameters
Dimension of robots	$l_1 = 1.6$, $l_2 = 1.2$.
Target for leader, centre	$(t_{11}, t_{12}) = (50, 10)$, and radius $rt_1 = 0.3$.
Final orientations	$t_{i3} = 0, \quad$ for $i = 1$ to 3.
Position of ghost targets	$(a_2, b_2) = (5, -5), \quad (a_3, b_3) = (-5, -5)$
Max. translational speed	$\upsilon_{max} = 5$.
Min. turning radius	$\rho_{min} = 0.14$.
Clearance parameter	$\epsilon_1 = 0.1$, $\epsilon_2 = 0.05$.
Coordinates for tunnel boundaries	$(q_{11}, r_{11}) = (20, 13)$, $(q_{12}, r_{12}) = (30, 13)$, $(q_{21}, r_{21}) = (20, 7)$, $(q_{22}, r_{22}) = (30, 7)$.
	Control and Convergence Parameters
Obstacle avoidance	$\alpha_{ik} = 0.001$, for $i =$1 to 3, $k = 1$ to 2.
Dynamics constraints	$\beta_{ij} = 0.01$ for $i, j = 1$ to 3, $i \neq j$.
Convergence	$\delta_{11} = 8$, $\delta_{12} = 2$, $\delta_{21} = 1$, $\delta_{22} = 2$, $\delta_{31} = 1$, $\delta_{32} = 2$.

facilitate tunnel passing (see Figure 5). Note the attraction functions from the leader-follower scheme ensures the members return to the prescribed formation within a predefined distance. Initially the follower-robots travel backwards to coalesce into the prescribed formation.

Figures 6 to 7 show the acceleration components of the individual robots of the team. One can clearly notice the convergence of the variables at the final state implying the effectiveness of the nonlinear controllers.

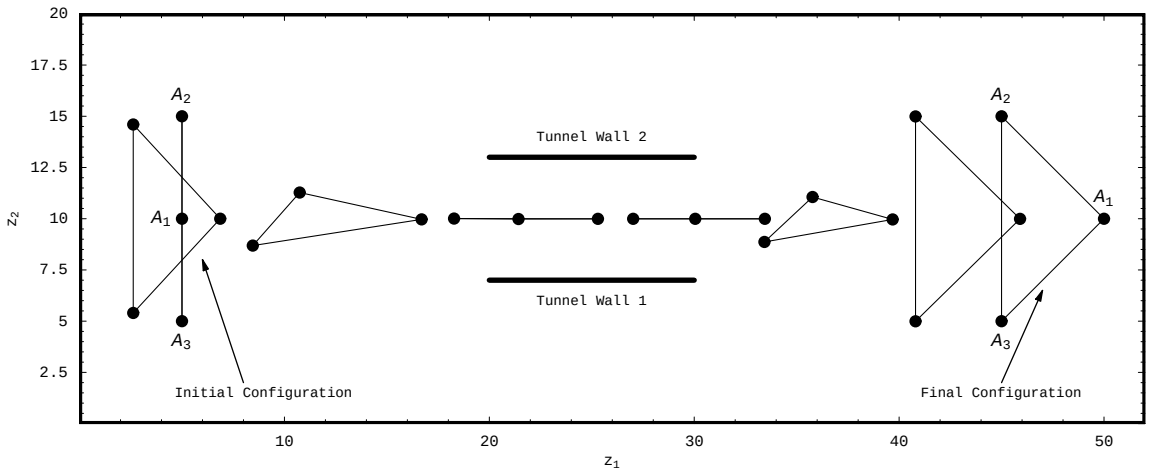

Fig. 5: The evolution of team trajectories to facilitate the split/rejoin maneuver for tunnel passing.

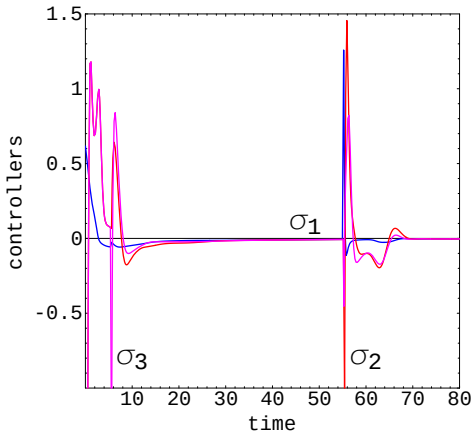

Fig. 6: Evolution of the translational accelerations of the team.

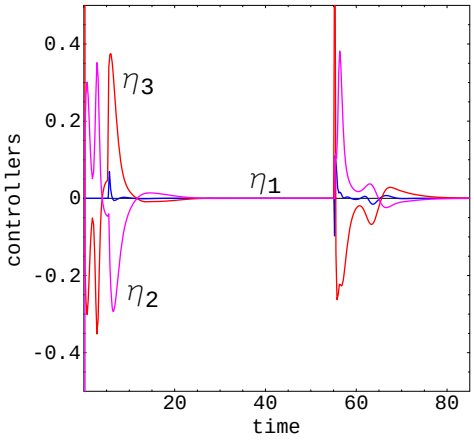

Fig. 7: Evolution of the rotational accelerations of the team.

6.2 Scenario 2: Expansion/Contraction

Assuming the units have been appropriately taken care of, initial conditions of the 3-robot team, obstacles and target configurations, limitation on velocities, and values of different parameters are given in Table 2, however, only those that are different from Scenario 1.

The control laws were implemented to generate feasible contraction/expansion maneuvers of the team to facilitate tunnel passing (see Figure 8). Note that while the attraction functions in the leader-follower scheme make sure that the team members return to the prescribed formation, the inter-robot bounds guarantee and maintain the shape of the formation although the size of the formation is continually changed. We also see that initially the follower-robots travel backwards to coalesce into the prescribed formation.

Figures 9 and 10 show the acceleration components of the team members. Once again we

Table 2: Numerical values of initial states, constraints and parameters for a simulation of Scenario 2.

	Constraints and Parameters
Maximum distance	$M_{12} = 8.4$, $M_{13} = 8.4$, $M_{21} = 8.4$, $M_{23} = 10.3$, $M_{31} = 8.4$, $M_{32} = 10.3$.
Minimum distance	$N_{ij} = 4.9$ for $i, j = 1$ to 3, $i \neq j$.
	Control and Convergence Parameters
Dynamics constraints	$\beta_{ij} = 3$ for $i, j = 1$ to 3, $i \neq j$.
Max. inter-robot bound	$\zeta_{ij} = 0.001$ for $i, j = 1$ to 3, $i \neq j$.
Min. inter-robot bound	$\xi_{ij} = 0.1$ for $i, j = 1$ to 3, $i \neq j$.
Convergence	$\delta_{11} = 10$, $\delta_{12} = 2$, $\delta_{21} = 1$, $\delta_{22} = 2$, $\delta_{31} = 1$, $\delta_{32} = 2$.

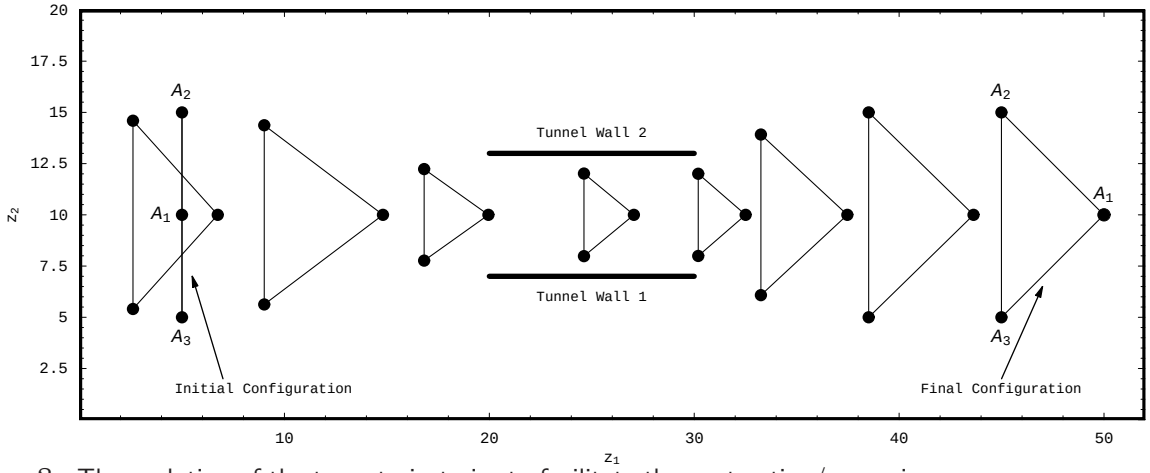

Fig. 8: The evolution of the team trajectories to facilitate the contraction/expansion maneuver.

clearly notice the convergence of the variables at the final state implying the effectiveness of the controllers. The velocity components share similar convergence trends.

7 Conclusions and Future Research

In this paper, the Lyapunov based control scheme provides a decentralized planning architecture which stands poised to tackle the tunnel passing problem in more than one possible way with its time invariant nonlinear controllers. The controllers enable a team of nonholonomic robots fixed in a prescribed formation to obtain collision-free tunnel passing maneuvers by deploying either split/rejoin or contraction/expansion of the formation. Inter alia, subtasks such as satisfying the nonholonomic and kinodynamic constraints associated with the system are also appropriately encompassed with the framework of the Lyapunov-based control scheme.

Although computationally intensive, the control scheme can invariably be extended to three-dimensional cases as well. All-in-all, the paper highlights a fairly broad conception that reflects at least some of the autonomy of swarms in nature. The Lyapunov function extracted

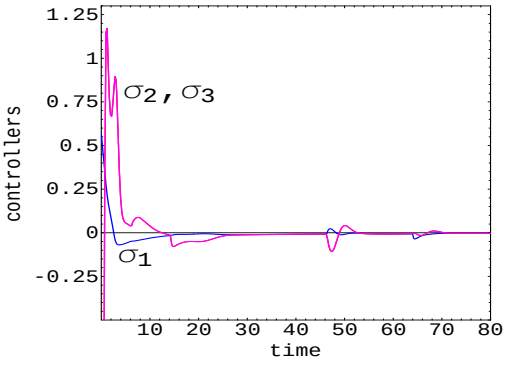

Fig. 9: Evolution of the translational accelerations of the team.

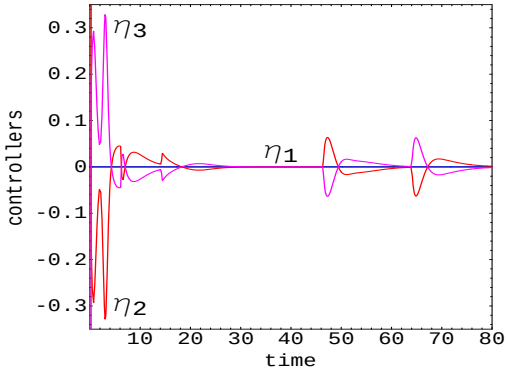

Fig. 10: Evolution of the rotational accelerations of the team.

from the control scheme also guaranteed stability of the system. Future work includes fine tuning the trajectories by parameter optimization, introducing curvature to the geometry of the tunnels and introducing non-leader strategies to the tunnel passing problem.

References

[1] A. Bazoula, M.S. Djouadi, and H. Maaref. Formation control of multi-robots via fuzzy logic technique. *International Journal of Computers, Communications and Control*, III:179–184, 2008.

[2] L. Consolini, F. Morbidi, D. Prattichizzo, and M. Tosques. Leader-follower formation control of nonholonomic mobile robots with input constraints. *Automatica*, 44:1343–1349, 2008.

[3] F. Morbidi and D. Prattichizzo. Sliding mode formation tracking control of a tractor and trailer-car system. In W. Burgard, O.Brock, and C. Stachniss, editors, *Robotics: Science and Systems III*, pages 126–133. MIT Press, 2008.

[4] B. Sharma, J. Vanualailai, and U. Chand. Flocking of multi-agents in constrained environments. *European Journal of Pure and Applied Mathematics*, 2(3):401–425, 2009.

[5] T. Ikeda, J. Jongusuk, T Ikeda, and T. Mita. Formation control of multiple nonholonomic mobile robots. *Electrical Engineering in Japan*, 157(3):81–88, 2006.

[6] F. Morbidi, G.L. Mariottini, and D. Prattichizzo. Observer design via immersion and invariance for vision-based leader-follower formation control. *AUTOMATICA*, September 2009.

[7] G.L. Mariottini, F. Morbidi, D. Prattichizzo, N. Vander Valk, N. Michael, G.J. Pappas, and K. Daniilidis. Vision-based localization for leader-follower formation control. *IEEE Transactions on Robotics*, August 2009.

[8] B. Sharma, J. Vanualailai, and A. Prasad. New collision avoidance scheme for multi-agents: A solution to the blindman's problem. *Advances in Differential Equations and Control Processes*, 3(2):141–169, 2009.

[9] C. Belta and V. Kumar. Abstraction and control for groups of robots. In *Reprinted from IEEE Transactions on Robotics and Automation*, volume 4, pages 865–875, October 2004.

[10] H. Freitas, P. Vilela, M. Ramalho, C. Cardeira, R. Loureiro, and J. Bengala. An industrial autonomous guided robot. In *Proceedings of the 16th Triennial IFAC World Congress*, Prague, July 2005.

[11] E. Frew and R. Sengupta. Obstacle avoidance with sensor uncertainty for small unmanned aircraft. In *43rd IEEE Conference on Decision and Control*, volume 1, pages 614–619, The Bahamas, 14-17 December 2004.

[12] R.T. Laird, M.H. Bruch, M.B. West, D.A. Ciccimaro, and H.R. Everett. Issues in vehicle teleoperation for tunnel and sewer reconnaissance. In *IEEE International Conference on Robotics and Automation*, San Francisco, CA, April 2000.

[13] J. Minguez. The obstacle-restriction method (ORM) for robot obstacle avoidance in difficult environments. In *Proceedings of the IEEE/RSJ International Conference on Intelligent Robots and Systems (IROS)*, pages 3706–3712, Edmonton, Canada, 2005.

[14] M. Peasgood, C. M. Clark, and J. McPhee. A complete and scalable strategy for coordinating multiple robots within roadmaps. *IEEE Transactions on Robotics*, 24(2):283–292, 2008.

[15] A. Shapiro, E. Rimon, and S. Shoval. A foothold selection algorithm for spider robot locomotion in planar tunnel environments. *The International Journal of Robotics Research*, 24(10):823–844, 2005.

[16] D. E. Chang, S. C. Shadden, J. E. Marsden, and R. Olfati-Saber. Collision avoidance for multiple agent systems. In *Procs. of the 42nd IEEE Conference on Decision and Control*, Maui, Hawaii USA, December 2003.

[17] R. Olfati-Saber. Flocking for multi-agent dynamic systems: Algorithms and theory. *IEEE Transactions on Automatic Control*, 51(3):401–420, 2006.

[18] R. Olfati-Saber and R. M. Murray. Flocking with obstacle avoidance: Cooperation with limited information in mobile networks. In *Procs. of the 42nd IEEE Conference on Decision and Control*, volume 2, pages 2022–2028, Maui, Hawaii, December 2003.

[19] B. Sharma. *New Directions in the Applications of the Lyapunov-based Control Scheme to the Findpath Problem*. PhD thesis, University of the South Pacific, Suva, Fiji Islands, July 2008. PhD Dissertation.

[20] O. Khatib. Real time obstacle avoidance for manipulators and mobile robots. *International Journal of Robotics Research*, 7(1):90–98, 1986.

[21] M. Ballerini, N. Cabibbo, R. Candelier, A. Cavagna, E. Cisbani, I. Giardina, V. Lecomte, A. Orlandi, G. Parisi, A. Procaccini, M. Viale, and V. Zdravkovic. Interaction ruling animal collective behavior depends on topological rather than metric distance: Evidence from a field study. In *Proceedings of the National Academy of Sciences of the United States of America*, volume 105, pages 1232–1237, January 2008.